

An Efficient Scaling Approach for Shape Based Image Compression

Jangam Ravi

Assistant Professor,

Avanthi's Scientific Technological & Research
Academy, Hyderabad.

Sravanvardhan Rao Souda

Assistant Professor,

Ellenki College of Engineering & Technology,
Hyderabad.

Abstract:

In this paper an approach to image compression based on shape based information is presented. The current shape based compression doesn't exploit the curvature information and basically uses the shape region information for compressing the image. In this paper an approach to compress the image based on the shape information exploiting the external shape variations in representative features for image compression. In this paper a curvature based scaling approach with wavelet transformation for image compression is presented.

Keyword:

Image compression, shape based approach, curvature scale spacing, wavelet transformation

I. INTRODUCTION:

Image compression remains a pure research objective in image processing from the evaluation of imaging applications. Various image compression algorithms were suggested in past with the objective of higher compression or better accuracy or both with regard to achieving compression for better accuracy all compression techniques were developed in lossy or lossless scheme. Where lossy schemes were proposed for compression architecture with high data rate, they compromise with obtained error limit. Various practical applications demands for high data rate compatibility with a error tolerance and in such system lossy compression where more suitable. System where accuracy is prime factor lossy compression schemes cannot be used. Lossless compression schemes are hence suggested. Digital imagery has had an enormous impact on industrial applications and scientific applications.

It is no surprise that image coding has been a subject of great commercial interest in today's world. The JPEG committee released a new image coding standard, JPEG 2000 which serves the enhancement to the existing JPEG system. The JPEG 2000 implements a new way of compressing images based on the wavelet transforms in contrast to the transformations used in JPEG standard. Generally an image is a positive function on a plane. The value of this function at each point specifies the luminance or brightness of the picture at that point. Digital images are sample versions of such functions, where the value of the function is specified only at discrete locations on the image plane, known as pixels. The value of the luminance at each pixel is represented to a predefined precision M . Eight bits of precision for luminance is common on imaging applications.

The eight-bit precision is motivated by both the existing memory structures (1 byte=8 bits) as well as the dynamic range of the human eye. The prevalent custom is that the samples (pixels) reside on a rectangular lattice, which will be assumed for convenience to be $N \times N$ matrix. The brightness value at each pixel is a number between 0 and 2^M-1 . The simplest binary representation of such an image is a list of the brightness values at each pixel, a list containing N^2M bits. In many image processing applications, exact reproduction of the image bits is not necessary. In this case, one can perturb the image slightly to obtain a shorter representation. If this perturbation is much smaller than the blurring and noise introduced in the formation of the image in the first place, there is no point in using the more accurate representation. Such a code procedure, where perturbations reduce storage requirements is known as Image lossy coding.

However to improve the time of transmission and the overall efficiency of system the Image is always compressed before transmission. There were various compression approaches and standards been suggested in past the most commonly used approach is the JPEG or JPG2K standards. Though these techniques are used for compression they are observed to be highly erroneous under noisy environment and are less accurate in retrieval due to noise effects and quantization effect. To improve the efficiency of such an method a compression approach based on shape information's were presented. Though most of the shape based compression approaches were made with the approach of edge information they may be very low in accuracy when compressed. To overcome this issue in this paper we present a shape based compression approach in variable environment using contour based curvature scale spacing approach in image compression.

II. SHAPE REPRESENTATION:

SHAPE representation is a pivotal step in shape analysis and matching systems. After the shape is located and segmented from an image, a representation technique is used to efficiently characterize the shape. The complexity and the performance of the subsequent steps in shape analysis systems are largely dependent on the invariance, robustness, stability, and uniqueness of the applied shape representation technique. In the past decade, several techniques have been proposed for 2D shape representation and matching. They include curvature scale space (CSS) [1], [2], [3], fuzzy-based matching [4], dynamic programming [5], shape contexts [6], shock graphs [7], geodesic paths [8], Fourier descriptors [9], and wavelet descriptors [10]. Objects can be recognized by their color, texture, and shape. Shape descriptors have become more popular, since they were adopted in the MPEG-7 system [11]. Region, contour, and skeleton shape descriptors were evaluated under the MPEG-7 system using a single-shape data set [12]. Generally, contour based descriptors performed significantly better than other category descriptors [13], [3].

Recent work in the area of extracting wavelet features which are invariant to geometric transformations has been very promising [14]. Wavelet analysis has become a powerful tool in several disciplines, including shape analysis and recognition [15], [16], [17]. Many researchers have adopted the Wavelet Transform (WT) in shape representation and matching. For example, WT was applied in 2D domains in [8], [9], [10], and [21], whereas WT was applied to 1D shape boundary in [12], [13], [14], and [10]. Due to the spatial and frequency localization property of the wavelet basis functions, wavelet descriptors are more efficient in representing and describing shapes than Fourier descriptors and moments [8]. The remainder of this paper is organized into the following sections: Section 2 is a brief overview of related research. In Sections 3 and 4, the proposed functions and the experimental results are presented, respectively. Last, the study is summarized and suggestions for future work are given.

III. CURVATURE SCALE SPACING:

The CSS technique is suitable for recovering invariant geometric features (curvature zero crossing points and/or extrema) of a planar curve at multiple scales. To compute it, the curve G is first parameterized by the arc length parameter u:

$$\Gamma(u) = (x(u), y(u))$$

An evolved version G_σ of G can then be computed.

$$\Gamma_\sigma = (X(u, \sigma), Y(u, \sigma))$$

Where $X(u, \sigma) = x(u) \otimes g(u, \sigma)$ $Y(u, \sigma) = y(u) \otimes g(u, \sigma)$

Where \otimes is the convolution operator and $g(u, \sigma)$ denotes a Gaussian of width σ . In order to find curvature zero – crossings or extrema from evolved versions of the input curve, one needs to compute curvature:

$$k(u) = \frac{X_u(u, \sigma)Y_{uu}(u, \sigma) - X_{uu}(u, \sigma)Y_u(u, \sigma)}{(X_u(u, \sigma)^2 + Y_u(u, \sigma)^2)^{1.5}}$$

Where,

$$\begin{aligned} X_u(u, \sigma) &= x(u) \otimes g_u(u, \sigma) & X_{uu}(u, \sigma) &= x(u) \otimes g_{uu}(u, \sigma) \\ Y_u(u, \sigma) &= y(u) \otimes g_u(u, \sigma) & Y_{uu}(u, \sigma) &= y(u) \otimes g_{uu}(u, \sigma) \end{aligned}$$

The corners are defined as the local maxima of the absolute value of curvature. At a very fine scale, there exist many such maxima due to noise and the digital contour. As the scale is increased, the noise is smoothed away and only the maxima corresponding to the real corners remain. The CSS corner-detection method finds the corners at these local maxima.

The process of CSS image corner detection is as follows:

Utilize the canny edge detector to extract edges from the original image.

Extract the edge contours from the image:

Fill the gaps in the edge contours.

Find the T – junctions and mark them as T – corners.

Compute the curvature at highest scale σ_{high} and determine the corner candidates by comparing the neighboring minima.

Track the corners to the lowest scale to improve localization.

Compare the T – corners to the corners found using the curvature procedure and remove corners which are very close.

These extracted contours were observed to be variant in spatial domain. The spatial resolution of the contour is exploited using a Discrete wavelet transformation.

IV. WAVELET APPROACH:

Digital image is represented as a two-dimensional array of coefficients, each coefficient representing the brightness level in that point. Differentiation can be made between coefficients as more important ones, and lesser important ones. Most natural images have smooth color variations, with the fine details being represented as sharp edges in between the smooth variations. Technically, the smooth variations in color can be termed as low frequency variations, and the sharp variations as high frequency variations.

The low frequency components (smooth variations) constitute the base of an image, and the high frequency components (the edges which give the details) add upon them to refine the image, thereby giving a detailed image. Hence, the smooth variations are more important than the details. Separating the smooth variations and details of the image can be performed in many ways. One way is the decomposition of the image using the discrete wavelet transform. Digital image compression is based on the ideas of sub-band decomposition or discrete wavelet transforms. Wavelets, which refer to a set of basic functions, are defined recursively from a set of scaling coefficients and scaling functions. The DWT is defined using these scaling functions and can be used to analyze digital images with superior performance than classical short-time Fourier-based techniques, such as the DCT, FFT.

The basic difference between wavelet-based and Fourier-based techniques is that short-time Fourier-based techniques use a fixed analysis window, while wavelet-based techniques can be considered using a short window at high spatial frequency data and a long window at low spatial frequency data. This makes DWT more accurate in analyzing image signals at different spatial frequency, and thus can represent more precisely both smooth and dynamic regions in image. A perfect reconstruction (PR) filter bank consists of filters that divide the input signal into subbands; the synthesis part of a PR filter bank reconstructs the original signal by recombining the subbands. The structure of a one dimensional (1-D), two channel PR filter bank is shown in Figure 2.2. $X(z)$ is the 1-D input signal. $H(z)$ and $G(z)$ are the z-transforms of the analysis lowpass and highpass filters; $F(z)$ and $J(z)$ are the z-transforms of the synthesis lowpass and highpass filters.

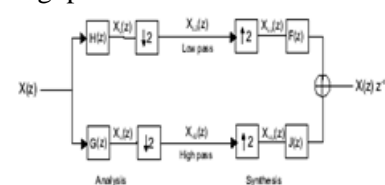


Figure 2.2: 1-D, 1 level PR filter bank

$H(z)$ and $G(z)$ split the input signal $X(z)$ into two subbands: lowpass ($XL(z)$) and highpass ($XH(z)$). The lowpass and highpass subbands are then downsampled generating $XLD(z)$ and $XHD(z)$ respectively. The upsampled signals, $XLU(z)$ and $XHU(z)$ are filtered by the corresponding synthesis lowpass ($F(z)$) and highpass ($J(z)$) filters and then added to reconstruct the original signal $X(z)$ that has an overall delay of d .

Although downsampling preserves the original sampling rate, it introduces aliasing since the magnitude response of the analysis filters are not ideal brickwall responses (they extend beyond their $\omega = \pi$ symmetry point). Apart from aliasing distortion, there are amplitude and phase distortions associated with the analysis filters. The synthesis filters are chosen to cancel the errors introduced by the analysis filters and the relation between the analysis and synthesis is given by the two PR conditions:

$$F(z)H(z) + J(z)G(z) = 2z^{fd}; \quad (1)$$

$$F(z)H(-z) + J(z)G(-z) = 0; \quad (2)$$

Equation (1) is called the 'no distortion' condition while Equation (2) is called the 'antialiasing' condition. The relation between the analysis and synthesis filters changes slightly for orthogonal and biorthogonal PR filter banks. In the case of an orthogonal PR filter bank, the synthesis filters are time reversed versions of the analysis filters: $F(z) = H(zf_1)$ and $J(z) = G(zf_1)$. Moreover, the highpass filter is the alternating ip of the lowpass filter, $G(z) = f_1 z^{N-1} H(f_1 z)$, where N is the length of the filter. Thus, the entire filter bank is defined by just one filter [the lowpass analysis filter $H(z)$]. In the case of a biorthogonal PR filter bank, the PR conditions are satisfied by choosing $G(z) = F(f_1 z)$ and $J(z) = f_1 H(f_1 z)$. Thus, the biorthogonal filter bank is defined by two filters $H(z)$ and $F(z)$. It is possible to obtain linear phase filters for biorthogonal wavelets unlike the case for orthogonal wavelets, where all the filters are derived from one filter $H(z)$. In this section, previously published papers in which the WT has been used to obtain affine invariant shape representations from its contour are reviewed.

Previous affine invariant wavelet-based shape boundary representations have been based on the detail coefficients, and the functions will be given next. Alferez and Wang [25] have proposed geometric and illumination invariants that depend on the wavelet detail coefficients for object recognition. Also, the authors have demonstrated that more complicated invariant functions can be constructed from more than two wavelet detail scale levels. Tieng and Boles have derived more than one affine invariant representation function by applying the dyadic WT to the contour of the shape. In [26], [27], Tieng and Boles have developed a relative invariant function from the approximation and detail coefficients of the shape contour that is mathematically expressed as

$$I_2(j, k) = D_j^1 \tilde{x}_k D_j^2 \tilde{y}_k - D_j^1 \tilde{y}_k D_j^2 \tilde{x}_k$$

where $A_i \tilde{x}_k$ are the approximation coefficients of the distorted boundary sequence \tilde{x}_k and $D_i \tilde{y}_k$ are the detail coefficients of the distorted boundary sequence \tilde{y}_k . For classification purposes, only the two levels with the highest energy concentrations are selected. Another invariant function was calculated by Tieng and Boles using the complex Daubechies wavelet functions. The real and imaginary parts of the detail coefficients have been used to compute this function.

By using the wavelet detail coefficients of two different wavelet functions, Tieng and Boles have developed another invariant function [29]. This function is given by

$$I_3(i, j, k) = D_i \tilde{x}_k D_j \tilde{y}_k - D_i \tilde{y}_k D_j \tilde{x}_k$$

where $D_i \tilde{x}_k$ are the approximation coefficients of the distorted boundary sequence \tilde{x}_k and $D_i \tilde{y}_k$ are the detail coefficients of the distorted boundary sequence \tilde{y}_k . For classification purposes, only the two levels with the highest energy concentrations are selected. Another invariant function was calculated by Tieng and Boles using the complex Daubechies wavelet functions. The real and imaginary parts of the detail coefficients have been used to compute this function. By using the wavelet detail coefficients of two different wavelet functions, Tieng and Boles have developed another invariant function.

This function is given by \tilde{y}_k are the detail coefficients of the distorted boundary at scale level j using the first wavelet transform and $D_{2j} \tilde{x}_k$ and $D_{2j} \tilde{y}_k$ are the detail coefficients of the distorted boundary after the second wavelet transform is applied at scale level j .

The framework for deriving affine invariant representation functions from the wavelet decomposition consists of the following steps:

The shape boundary (sometimes called the shape outer contour) is found and extracted by using one of the known boundary tracing techniques (the 8-connectivity technique is used in this work). The parameterized shape boundary $c_k \frac{1}{4} \frac{1}{2} x_k; y_k$ is split into two 1D sequences, x_k and y_k . For a 2D shape represented by its contour parametric equation (sequences x_k and y_k) and subjected to an affine transformation, the relation between the original and the distorted sequences is given by

$$\begin{bmatrix} \tilde{x}_k \\ \tilde{y}_k \end{bmatrix} = \begin{bmatrix} c_{11} & c_{12} \\ c_{21} & c_{22} \end{bmatrix} \begin{bmatrix} x_k \\ y_k \end{bmatrix} + \begin{bmatrix} b_1 \\ b_2 \end{bmatrix}$$

where \tilde{x}_k, \tilde{y}_k are the affine distorted sequences $c_{11}, c_{12}, c_{21},$ and c_{22} denote the affine matrix coefficients, and b_1 and b_2 represent the translation parameters. The effect of the translation parameters is easily reduced by normalizing the shape boundary centroid. The normalization is completed by subtracting the mean value of the boundaries from their extracted values. From the wavelet multiresolution analysis properties, and for any function $f \in L^2(\mathbb{R}^2)$, f can be expressed by the approximation and detail wavelet coefficients

$$f(k) = \sum_n A_{J,n} \phi_{J,n}(k) + \sum_{j=j_0}^J \sum_n D_{j,n} \psi_{j,n}(k) \quad J > j_0$$

where $A_{J,n}$ are the approximation coefficients at scale level J , $\phi_{J,n}$ is the scaling function, $D_{j,n}$ are the detail coefficients at scale level j , $\psi_{j,n}$ is the wavelet function, and j_0 is the finest decomposed scale level. For simplicity, the wavelet coefficients will be written without the suffix n (e.g., $A_{j,n}$ and $D_{j,n}$ will be denoted as A_j and D_j , respectively).

If the WT is applied to the affine distorted shape boundary, then the wavelet transformed shape boundary is affected by the same affine transformations. This occurs because the WT is a linear transform and the same affine transformation exists in the wavelet domain (after the translation effect has been removed). For the two different representations of x_k and y_k (i.e., by using either different scale levels or two types of different coefficients), all the wavelet coefficients (in all the scale levels) are subjected to the same geometric transformation,

$$\begin{bmatrix} WT_i \tilde{x}_k & WT_j \tilde{x}_k \\ WT_i \tilde{y}_k & WT_j \tilde{y}_k \end{bmatrix} = \begin{bmatrix} c_{11} & c_{12} \\ c_{21} & c_{22} \end{bmatrix} \begin{bmatrix} WT_i x_k & WT_j x_k \\ WT_i y_k & WT_j y_k \end{bmatrix}$$

An affine invariant function is computed by taking the determinant of (6), which is

$$\begin{aligned} & WT_i \tilde{x}_k WT_j \tilde{y}_k - WT_i \tilde{y}_k WT_j \tilde{x}_k = \\ & \det(C)(WT_i x_k WT_j y_k - WT_i y_k WT_j x_k) \end{aligned}$$

where C is the transformation matrix. Most of the previously derived affine invariant representation functions can be computed from (7). These invariant functions are computed by selecting the wavelet coefficients WTx_k and WTy_k as either the wavelet detail coefficients or the approximation and detail coefficients.

V. SIMULATION RESULTS:

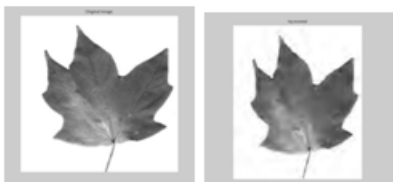
Two of the error metrics used to compare the various image compression techniques are the Mean Square Error (MSE) and the Peak Signal to Noise Ratio (PSNR). The MSE is the cumulative squared error between the compressed and the original image, whereas PSNR is a measure of the peak error. The mathematical formulae for the two are

$$MSE = \frac{1}{MN} \sum_{Y=1}^M \sum_{X=1}^N [I(x,y) - I'(x,y)]^2$$

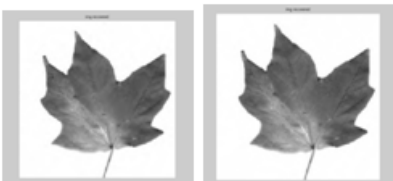
$$PSNR = 20 * \log_{10} (255 / \sqrt{MSE})$$

where $I(x,y)$ is the original image, $I'(x,y)$ is the approximated version (which is actually the decompressed image) and M,N are the dimensions of the images.

A lower value for MSE means lesser error, and as seen from the inverse relation between the MSE and PSNR, this translates to a high value of PSNR. Logically, a higher value of PSNR is good because it means that the ratio of Signal to Noise is higher. Here, the 'signal' is the original image, and the 'noise' is the error in reconstruction. So, if you find a compression scheme having a lower MSE (and a high PSNR), you can recognise that it is a better one



(a) Original leaf image sample
(b) Recovered image at 0.1 bpp



(c) Recovered image at 0.5 bpp
(d) Recovered image at 0.9 bpp



(a) Original flower image sample
(b) Recovered flower image sample at 0.1 bpp



(c) Recovered flower image sample at 0.5 bpp
(d) Recovered flower image sample at 0.9 bpp

VII. CONCLUSION:

In this paper a shape based compression scheme with the incorporation of shape information with spectral wavelet coefficients. The wavelet information exploits the resolution information of the given shape image and its relational information of distribution with contour level distribution. The obtained image is evaluated for the PSNR value at different bit coding and observed to be at higher retrieving accuracy at higher bit per pixel representation. This paper provides a low computational shape based wavelet based compression approach for image compression.

VIII. REFERENCES:

- [1] G. Qiu. Colour image indexing using BTC. IEEE Trans. Image Processing, 12(1):93{101, 2003.
- [2] G. Schaefer, G. Qiu, and M.R. Luo. Visual pattern based colour image compression. In Visual Communication and Image Processing 1999, volume 3653 of Proceedings of SPIE, pages 989{997, 1999.
- [3] G. Schaefer and M. Stich. UCID - An Uncompressed Colour Image Database. In Storage and Retrieval Methods and Applications for Multimedia 2004, volume 5307 of Proceedings of SPIE, 2004.
- [4] R.O. Stehling, M.A. Nascimento, and A.X. Falcao. A compact and efficient image retrieval approach based on border/interior pixel classification. In Proc. 11th Int. Conf. on Information and Knowledge Management, pages 102{109, 2002.
- [5] M.J. Swain and D.H. Ballard. Color indexing. Int.J. Computer Vision, 7(11):11{32, 1991.
- [6] M. Khalil and M. Bayoumi, "Affine Invariant Object Recognition Using Dyadic Wavelet Transform," Proc. 2000 Canadian Conf. Electrical and Computer Eng., vol. 1, pp. 421-425, 2000.
- [7] M. Khalil and M. Bayoumi, "Affine Invariants for Object Recognition Using the Wavelet Transform," Pattern Recognition Letters, vol. 23, pp. 57-72, 2002.



[8] M. Khalil and M. Bayoumi, "A Dyadic Wavelet Affine Invariant Function for 2-D Shape Recognition," IEEE Trans. Pattern Analysis and Machine Intelligence, vol. 23, no. 10, pp. 1152-1164, Oct. 2001.

[9] E. Bala and A. Cetin, "Computationally Efficient Wavelet Affine Invariant Functions for Shape Recognition," IEEE Trans. Pattern Analysis and Machine Intelligence, vol. 26, no. 8, pp. 1095-1099, Aug. 2004.

[10] An Introduction to Wavelets, vol. 1 of Wavelet Analysis and Its Applications, C. Chui, ed. Academic Press, 1992.

[11] Wavelet Theory and Its Application to Pattern Recognition, vol. 36 of Machine Perception and Artificial Intelligence, Y. Tang, L. Yang, J. Liu, and H. Ma, eds. World Scientific, 2000.

[12] E. Petrakis, A. Diplaros, and E. Milios, "Matching and Retrieval of Distorted and Occluded Shapes Using Dynamic Programming," IEEE Trans. Pattern Analysis and Machine Intelligence, vol. 24, no. 11, pp. 1501-1516, Nov. 2002.

[13] S. Belongie, J. Malik, and J. Puzicha, "Shape Matching and Object Recognition Using Shape Contexts," IEEE Trans. Pattern Analysis and Machine Intelligence, vol. 24, no. 24, pp. 509-522, Apr. 2002.

[14] T. Sebastian, P. Klein, and B. Kimia, "Recognition of Shapes by Editing Their Shock Graphs," IEEE Trans. Pattern Analysis and Machine Intelligence, vol. 26, no. 5, pp. 550-571, May 2004.

[15] E. Klassen, A. Srivastava, W. Mio, and S. Joshi, "Analysis of Planar Shapes Using Geodesic Paths on Shape Spaces," IEEE Trans. Pattern Analysis and Machine Intelligence, vol. 26, no. 3, pp. 372-383, Mar. 2004.